

## LARGE-SCALE STRUCTURE OF THE CARINA NEBULA

NATHAN SMITH,<sup>1</sup> MICHAEL P. EGAN,<sup>2</sup> SEAN CAREY,<sup>3</sup> STEPHAN D. PRICE,<sup>2</sup> JON A. MORSE,<sup>4</sup> AND PAUL A. PRICE<sup>5</sup>

Received 1999 November 17; accepted 2000 February 7; published 2000 March 7

### ABSTRACT

Observations obtained with the *Midcourse Space Experiment* (*MSX*) satellite reveal for the first time the complex mid-infrared morphology of the entire Carina Nebula (NGC 3372). On the largest size scale of  $\sim 100$  pc, the thermal infrared emission from the giant H II region delineates one coherent structure: a (somewhat distorted) bipolar nebula with the major axis perpendicular to the Galactic plane. The Carina Nebula is usually described as an evolved H II region that is no longer actively forming stars, clearing away the last vestiges of its natal molecular cloud. However, the *MSX* observations presented here reveal numerous embedded infrared sources that are good candidates for sites of current star formation. Several compact infrared sources are located at the heads of dust pillars or in dark globules behind ionization fronts. Because their morphology suggests a strong interaction with the peculiar collection of massive stars in the nebula, we speculate that these new infrared sources may be sites of triggered star formation in NGC 3372.

*Subject headings:* H II regions — ISM: individual (Carina Nebula) — stars: formation

### 1. INTRODUCTION

The Carina Nebula (NGC 3372) harbors one of the most remarkable aggregates of unusually massive stars known in the Galaxy, including the young clusters Trumpler 14, 15, and 16, Collinder 228 and 232, and Bochum 10 and 11. Together, these clusters contain at least 64 O-type stars and two Wolf-Rayet stars—the remnants of a burst of star formation that ended  $\sim 3$  Myr ago. The stellar content of the Carina Nebula has been discussed extensively in the literature (e.g., Walborn 1971, 1973, 1995; Massey & Johnson 1993; Feinstein 1995; Davidson & Humphreys 1997); most notable are the rare main-sequence O3 stars, the O3 supergiant HD 93129A, and, of course, the peculiar object  $\eta$  Carinae.

That the young massive stars in NGC 3372 are associated with gas and dust has been known for some time because of the bright nebulosity and prominent dust lanes in optical photographs of the region. Most studies of the large-scale structure in the nebula focus on the central  $\sim 0.5$  deg<sup>2</sup> containing Tr 14 and 16, the Keyhole Nebula, and the dark V-shaped dust lanes that obscure part of the bright nebulosity. Far-infrared and molecular radio surveys of the region (Harvey, Hoffmann, & Campbell 1979; Gosh et al. 1988; de Graauw et al. 1981) suggest that NGC 3372 is an evolved H II region, with dust and neutral gas evacuated from its core, and that Carina lacks the compact, high-density, embedded star-forming cores that are common in other young Galactic H II regions such as W49 and W51. Ongoing star formation has been suggested for only one relatively inconspicuous source in the nebula, IRAS 10430–5931 (Megeath et al. 1996).

The mid-IR images presented here combine the advantages of a large field of view ( $\sim 12$  deg<sup>2</sup>) and spatial resolution ( $18''$ ) several times better than *IRAS* or the far-IR and molecular surveys discussed above. The *Midcourse Space Experiment*

(*MSX*) data demonstrate that IRAS 10430–5931 is just one of many IR condensations, most of which are outside the central core of the nebula. These are good candidates for sites of current active star formation, with a triggering mechanism analogous to the scenario discussed by Elmegreen & Lada (1977). Consequently, the discovery of these IR condensations alters the current understanding of NGC 3372 as an evolved H II region without active star formation.

### 2. OBSERVATIONS AND RESULTS

The Carina Nebula was observed by the *MSX* satellite, which is a Ballistic Missile Defense Organization satellite launched in 1996 April that is equipped with a 33 cm diameter telescope and an IR imager called SPIRIT III. Details of the instrumentation (sensitivity, scan rate, calibration, etc.) are given by Egan et al. (1998), and a description of the astronomical experiments on *MSX* is given by Price (1995). Figure 1*a* shows the *MSX* band A ( $\Delta\lambda = 6.8$ – $10.8$   $\mu$ m) data presented in false color with the horizontal direction parallel to the Galactic plane. Diffuse areas in band A are most likely dominated by emission from cationic polycyclic aromatic hydrocarbons (PAHs; see Allamandola, Hudgins, & Sanford 1999) in photodissociation regions on the surfaces of molecular clouds, although the point sources may be thermal dust emission. The object  $\eta$  Car is the brightest mid-IR source in the region and is located in the core of the nebula (marked with a cross in Figs. 1 and 2). The pixel scale of the *MSX* band A image in Figure 1*a* is  $18''$ , which undersamples the diffraction limit of the telescope at  $\lambda = 8$   $\mu$ m ( $\sim 6''$ ).

To compare the spatial distribution of mid-IR emission in the *MSX* images with that of ionized gas, we also present wide-field optical emission line images in the light of [O III]  $\lambda 5007$ , H $\alpha$ , and [S II]  $\lambda\lambda 6716, 6731$  obtained in 1999 April as part of the Mount Stromlo and Siding Spring Observatories (MSSSO) H $\alpha$  Survey. The survey uses an f/4.5 Nikkor-Q lens and a SITE-thinned  $2k \times 2k$  CCD, with a pixel scale of  $\sim 12''$  (Buxton, Bessell, & Watson 1998). Figure 1*b* shows a composite three-color image of ionized gas in NGC 3372, constructed with the optical MSSSO H $\alpha$  Survey images. The orientation and field of view are identical to Figure 1*a*. The gray-scale image in Figure 2 shows the variation of the H $\alpha$ -to-*MSX* band A emission ratio across the nebula. In Fig-

<sup>1</sup> Department of Astronomy, University of Minnesota, 116 Church Street, SE, Minneapolis, MN 55455; nathans@astro.umn.edu.

<sup>2</sup> US Air Force Research Laboratory, VSBC, 29 Randolph Road, Hanscom AFB, MA 01731-3010.

<sup>3</sup> Institute for Scientific Research, Boston College, Chestnut Hill, MA 02167.

<sup>4</sup> Center for Astrophysics and Space Astronomy, University of Colorado, Campus Box 389, Boulder, CO 80309.

<sup>5</sup> Research School of Astronomy and Astrophysics, Australian National University, Private Bag, Weston Creek P.O., Canberra, ACT 2611, Australia.

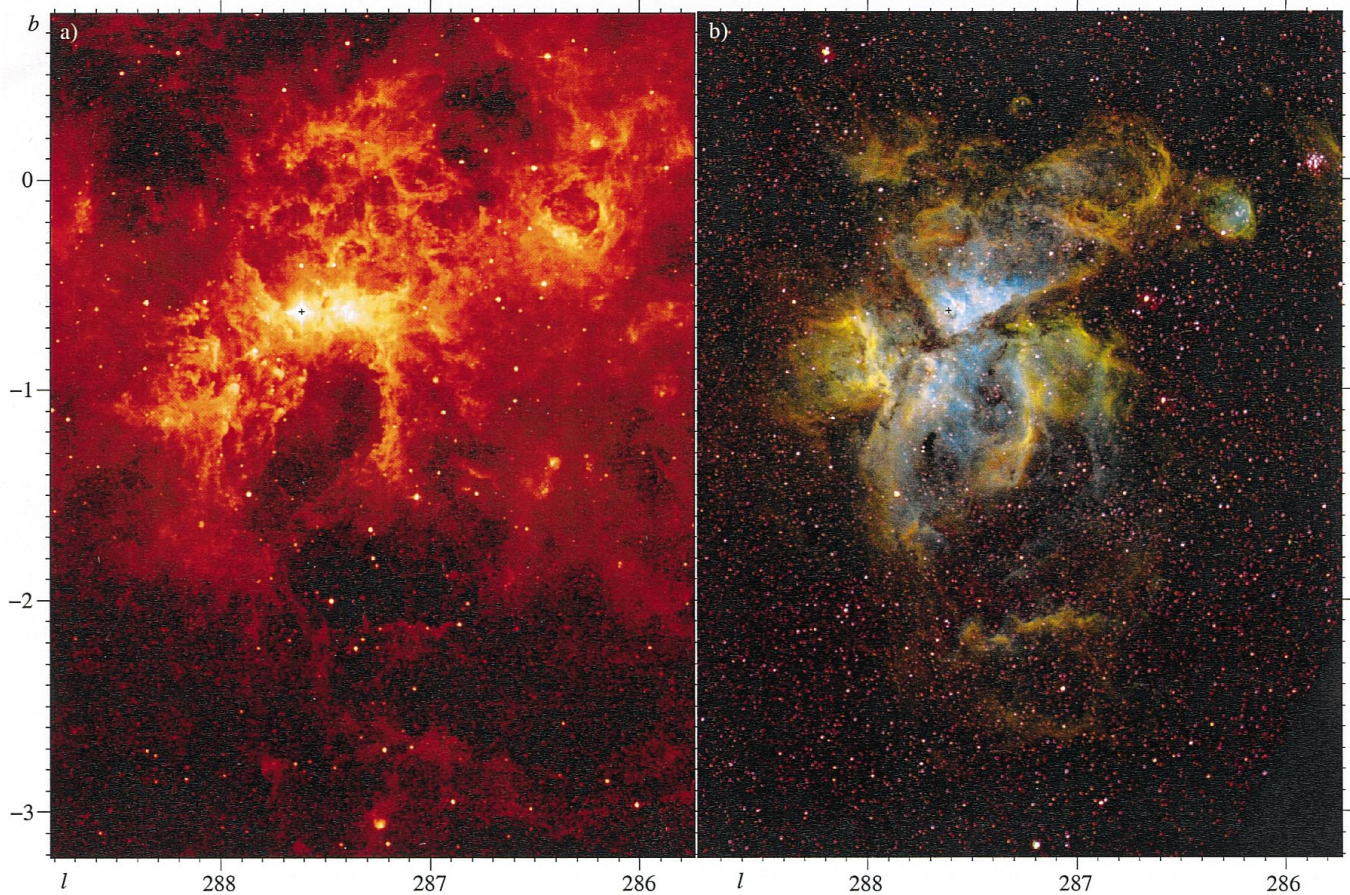


FIG. 1.—(a) False-color image of the Carina Nebula using the MSX band A data (6.8–10.8  $\mu\text{m}$ ). The logarithmic color scale has irradiance values that range from  $5 \times 10^{-12}$  (black) to  $5 \times 10^{-8}$   $\text{W cm}^{-2} \text{sr}^{-1}$  (white). (b) Composite three-color optical image of ionized gas in NGC 3372. Blue represents [O III]  $\lambda 5007$  emission, green is  $\text{H}\alpha$ , and red indicates [S II]  $\lambda\lambda 6716, 6731$  emission; (a) and (b) have the same field of view, and the axes are labeled in degrees of Galactic longitude  $l$  and latitude  $b$ . The position of  $\eta$  Car is marked with a black cross in both panels.

ure 2, areas with strong mid-IR emission are dark, and ionized gas is light.

### 3. DISCUSSION

#### 3.1. A Bipolar Superbubble?

Figure 1 suggests that on the largest scale, the Carina Nebula has a bipolar structure that is pinched at the waist by cold dust and gas. The major axis appears to be nearly perpendicular to the Galactic plane. The bipolar lobes have diameters of  $\sim 1^\circ$  (40 pc, assuming  $d = 2.3$  kpc), although they are not simple spherical shells. The interiors of these lobes show [O III] emission in Figure 1b, and they are outlined by  $\text{H}\alpha$  and [S II] filaments. The polar lobe that extends toward  $+b$  appears to be impacting the Galactic plane, and the prominent lobe extending toward  $-b$  appears to be one in a sequence of large shells that reach as far as  $\sim 2.7$  (110 pc) from the core of the nebula. The bipolarity of NGC 3372 suggests that expansion along the Galactic plane has been inhibited by high-density molecular gas. This, in turn, suggests that the original molecular cloud may have had a flattened distribution aligned with the Galactic plane, in agreement with the results of Hopper & Disney (1974) for a large sample of Galactic dark clouds. If we take 110 pc as the maximum expansion radius that the H II region would achieve if it were expanding in a homogeneous interstellar medium with  $n_0 = 1 \text{ cm}^{-3}$ , we can approxi-

mate the energy input needed to shape the nebula since it can be shown for an expanding shell that the kinetic energy of the displaced atomic hydrogen mass is  $E = 8.62 \times 10^{53} n_0 R_{\text{pc}}^5 t_{\text{yr}}^{-2}$  ergs (assuming a constant expansion velocity  $v = R_{\text{pc}}/t_{\text{yr}}$ ), where  $n_0$  is the ambient hydrogen density in units of  $\text{cm}^{-3}$ ,  $R_{\text{pc}}$  is the characteristic expansion radius in parsecs, and  $t_{\text{yr}}$  is the age in years. An age of  $3 \times 10^6$  yr corresponding to the most evolved objects in NGC 3372 ( $\eta$  Car and the Wolf-Rayet stars; Davidson & Humphreys 1997) gives a kinetic energy of  $\sim 1.5 \times 10^{51}$  ergs. If we instead use the self-similar expression  $E = 5.3 \times 10^{43} n_0^{1.12} R_{\text{pc}}^{3.12} v^{1.4}$  ergs (Chevalier 1974) for this parameter and  $v = R/t \approx 35 \text{ km s}^{-1}$ , we derive a larger value of  $8.8 \times 10^{51}$  ergs. These estimates for the amount of energy are comparable to those derived by similar methods for large-scale H II shells in the Galaxy (Heiles 1979) and are comparable to the canonical value for the kinetic energy of one or more supernova explosions. However, the expansion of NGC 3372 is primarily due to stellar winds and radiation since no conclusive evidence for any supernova remnants has been found there (Retallack 1983; Lopez & Meaburn 1984; Whiteoak 1994).

Throughout the nebula, including the most extended regions, the stratified ionization fronts (Fig. 1b) are consistent with ionization by the clusters of massive stars in the core of the nebula (primarily Tr 14 and 16). The ionized filaments are delineated by diffuse [O III] emission, followed by  $\text{H}\alpha$  and [S II] with increasing distance from Tr 16 (except NGC 3324, which has

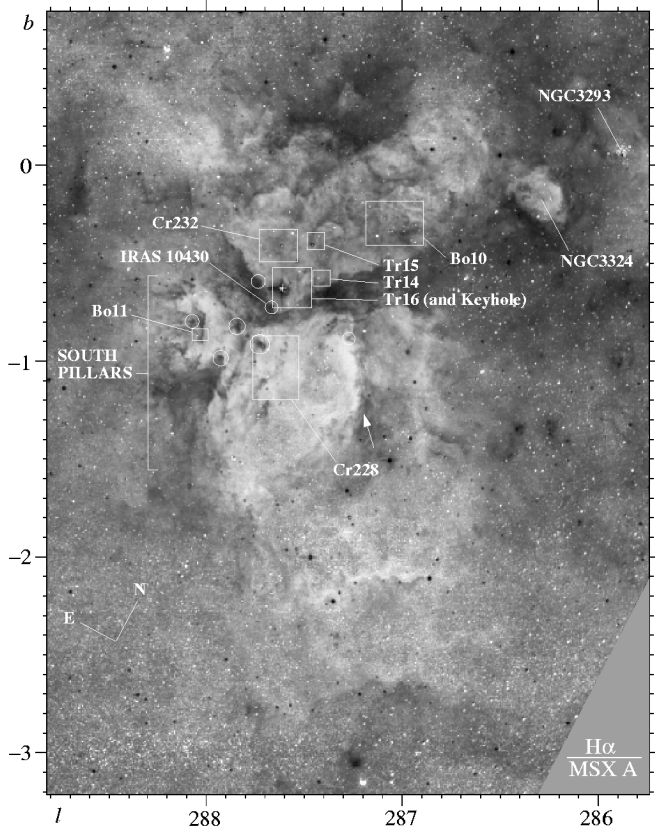


FIG. 2.— $H\alpha$ -to- $MSX$  band A flux ratio image. This map shows the relative spatial distribution of ionized gas (*bright areas*) and mid-IR PAH emission and compact IR sources (*dark areas*). The boxes denote approximate locations of massive star clusters, and the circles identify a few of the most striking embedded IR sources (see Table 1). The position of  $\eta$  Car is marked with a white cross, and the edge-on ionization front referred to in § 3.1 is identified by the white arrow.

its own ionization source). This stratification in edge-on ionization fronts is expected in a photoionized, photoevaporative flow (Bertoldi 1989). Furthermore, emission from ionized PAHs is located at larger distances from the ionizing stars than the  $H\alpha$  and  $[S\ II]$  emission (most clearly demonstrated by the 0.5-long edge-on ionization front in the center of Fig. 2), indicating that the  $H\ II$  region also contains large-scale photo-dissociation regions and that the ionizing radiation and stellar winds from the massive stars in the center of the Carina Nebula are shaping the interstellar medium over a region  $\sim 175$  pc in extent by accelerating the ambient molecular gas (e.g., Oort & Spitzer 1955).

### 3.2. Filamentary Structure

The polar lobe extending toward  $+b$  is characterized by a complex network of filamentary arcs and shells in Figures 1a and 1b. The morphology of this region gives the impression that the  $H\ II$  region is expanding into a highly structured, porous interstellar medium and that the observed features may be due to density inhomogeneities in the ambient medium. Many of the bright IR filaments are coincident with dark regions in Figure 1b and lie adjacent to optical ionization fronts (Fig. 2). Inside the upper polar lobe is a bright cometary or teardrop-shaped mid-IR feature that appears to “drip” down toward the core of the nebula (located at  $l, b \approx 287.44, -0.41$ ), the bright “head” of which is suspiciously close to Tr 15. In contrast to

the upper polar lobe, the expansion toward  $-b$  is composed of a set of large, limb-brightened, thin shells that do not imply a similar porous structure for the ambient medium. The smallest of these shells is the most striking and corresponds to the lower polar lobe discussed above; the outer shells are fainter and extend to the lower right in Figure 1. The images give the impression that these shells overlap near the core of the nebula and are expanding with one shell inside (or behind) another. The thickness of these shell walls is on the order of 0.1 (4 pc).

### 3.3. Triggered Star Formation

At various positions around the periphery of the nebula, IR-bright condensations can be seen as clumps, protrusions, or corrugations in the walls of the  $H\ II$  region. Many of these IR sources are coincident with bright-rimmed globules found in edge-on ionization fronts (Fig. 2). Typical sizes of these globules are on the order of 1 pc, and typical separations between globules along a given filament are  $\sim 5$  pc. Since most of these mid-IR sources lie in swept-up neutral regions directly behind ionization fronts, they are good candidates for sites of triggered star formation via the scenario discussed by Elmegreen & Lada (1977). One of these sources is the bright-rimmed globule IRAS 10430–5931, which thus far has been the only proposed site of ongoing (and triggered) star formation in NGC 3372 (Megeath et al. 1996). IRAS 10430–5931 is located just behind an ionization front in one of the prominent dark dust lanes that appear to bisect the middle of the  $H\ II$  region (Figs. 1b and 2). Many other IR sources revealed by  $MSX$  show a morphology similar to IRAS 10430–5931, especially several clumps along the edge of the dark cloud to the east of  $\eta$  Car, which includes IRAS 10430–5931. The location of these IR globules at the periphery of the nebula behind ionization fronts (Fig. 2) that are obviously interacting with nearby massive stars vividly demonstrates the *collect-and-collapse* phase in the scenario of intermediate-scale-triggered star formation discussed by Elmegreen (1992). In this scenario, the  $MSX$  globules may have formed as a result of thin layer instabilities in an accelerating sheet of swept-up neutral gas and dust.

### 3.4. The South Pillars

Roughly 0.5 south of  $\eta$  Car (to the lower left of  $\eta$  Car in Fig. 1) is a remarkable region containing several elongated dust pillars, the largest and brightest of which is  $\sim 25$  pc long and seems to point toward  $\eta$  Car. This giant dust pillar in Carina is more than an order of magnitude larger than dust pillars observed in 30 Doradus and Galactic  $H\ II$  regions and is coincident with an unresolved molecular cloud (Grabelsky et al. 1988). The pillars generally have bright heads on the side facing toward  $\eta$  Car and elongated tails pointing away from it, suggesting that the stellar winds and ionizing radiation from  $\eta$  Car and the other members of Tr 16 have been largely responsible for sculpting this region (note that the cometary tails do not point away from the nearest cluster in the plane of the sky, Bo 11). In Figure 1b, these structures appear as dark columns with bright rims in the light of  $H\alpha$  and  $[S\ II]$  and are reminiscent of the features observed in 30 Dor that point toward R136 (Walborn et al. 1999). Walborn et al. suggest that these structures in 30 Dor are prime candidates for triggered *massive* star formation, and this may also be the case in the Carina Nebula. If the heads of these dust pillars do harbor newly forming stars, we should expect them to be complex near- and mid-IR sources, worthy of further investigation at higher resolution. Some of the most striking mid-IR sources are circled in Figure 2 and



listed in Table 1, where the names of the sources correspond to their Galactic coordinates (Table 1 also includes a few sources of the sort discussed in § 3.3). These sources were selected for their location behind edge-on ionization fronts and their bright and compact mid-IR emission (making them good candidates for ground-based observations). Numerous other candidates will be given in a forthcoming paper. These candidates may be useful in planning upcoming mid- and far-IR or submillimeter observations.

The region containing the south pillars (see Fig. 2) is not included in the field of the far-IR and molecular studies by Harvey et al. (1979), Gosh et al. (1988), and de Graauw et al. (1981), which may explain why these authors conclude that NGC 3372 is an evolved H II region without active star formation. Long-wavelength investigations of the Carina Nebula during the past decade (e.g., Cox 1995; Megeath et al. 1996) also cover only the central region of the nebula and verify these conclusions; Cox (1995) even comments on the apparent paucity of embedded IR sources in Carina. The complex of IR sources in the south pillar region discovered by *MSX* drastically

TABLE 1  
COMPACT IR SOURCES<sup>a</sup>

Name	$\alpha(2000)$	$\delta(2000)$
G287.28–0.88 .....	10 41 54	–59 45 21
G287.73–0.59 .....	10 46 08	–59 42 41
G287.73–0.92 .....	10 44 55	–60 00 13
G287.84–0.82 .....	10 46 04	–59 57 58
G287.93–0.99 .....	10 46 05	–60 09 30
G288.07–0.80 .....	10 47 47	–60 03 15

NOTE.—Units of right ascension are hours, minutes, and seconds, and units of declination are degrees, arcminutes, and arcseconds.

<sup>a</sup> Coordinates are approximate since sources typically cover more than 18" (1 pixel).

changes this view of the Carina Nebula, indicating the importance of large field-of-view IR observations. We speculate that the south pillars represent the next generation of star formation in NGC 3372. A future paper will investigate the truth of this speculation in more detail, but new observations of this region are strongly encouraged.

#### REFERENCES

- Allamandola, L. J., Hudgins, D. M., & Sanford, S. A. 1999, *ApJ*, 511, L115  
 Bertoldi, F. 1989, *ApJ*, 346, 735  
 Buxton, M., Bessell, M., & Watson, R. 1998, *Publ. Astron. Soc. Australia*, 15, 24  
 Chevalier, R. A. 1974, *ApJ*, 188, 501  
 Cox, P. 1995, *Rev. Mexicana Astron. Astrofis. Ser. Conf.*, 2, 105  
 Davidson, K., & Humphreys, R. M. 1997, *ARA&A*, 35, 1  
 de Graauw, T., et al. 1981, *A&A*, 102, 257  
 Egan, M. P., Shipman, R. F., Price, S. D., Carey, S. J., Clark, F. O., & Cohen, M. 1998, *ApJ*, 494, L199  
 Elmegreen, B. G. 1992, in *Star Formation in Stellar Systems*, ed. G. Tenorio-Tagle et al. (Cambridge: Cambridge Univ. Press), 381  
 Elmegreen, B. G., & Lada, C. J. 1977, *ApJ*, 214, 725  
 Feinstein, A. 1995, *Rev. Mexicana Astron. Astrofis. Ser. Conf.*, 2, 57  
 Ghosh, S. K., et al. 1988, *ApJ*, 330, 928  
 Grabelsky, D. A., Cohen, R. S., Bronfman, L., & Thaddeus, P. 1988, *ApJ*, 331, 181  
 Harvey, P. M., Hoffmann, W. F., & Campbell, M. F. 1979, *ApJ*, 227, 114  
 Heiles, C. 1979, *ApJ*, 229, 533  
 Hopper, P. B., & Disney, M. J. 1974, *MNRAS*, 168, 639  
 Lopez, J. A., & Meaburn, J. 1984, *Rev. Mexicana Astron. Astrofis.*, 9, 119  
 Massey, P., & Johnson, J. 1993, *AJ*, 105, 980  
 Megeath, S. T., Cox, P., Bronfman, L., & Roelfsema, P. R. 1996, *A&A*, 305, 296  
 Oort, J. H., & Spitzer, L. 1955, *ApJ*, 121, 60  
 Price, S. D. 1995, *Space Sci. Rev.*, 74, 81  
 Retallack, D. S. 1983, *MNRAS*, 204, 669  
 Walborn, N. R. 1971, *ApJ*, 167, L31  
 ———. 1973, *ApJ*, 179, 517  
 ———. 1995, *Rev. Mexicana Astron. Astrofis.*, 2, 51  
 Walborn, N. R., et al. 1999, *AJ*, 117, 225  
 Whiteoak, J. B. Z. 1994, *ApJ*, 429, 225